Co-published by
Institute of Fluid-Flow Machinery
Polish Academy of Sciences
Committee on Thermodynamics and Combustion
Polish Academy of Sciences

Copyright©2026 by the Authors under licence CC BY-NC-ND 4.0

http://www.imp.gda.pl/archives-of-thermodynamics/

Analysis of phase behaviour of R1243zf/lubricant oil mixtures and its impact on the performance of vapour-compression refrigeration cycle

Heyu Jia, Wenzhe Dang, Xiaopo Wang*

Key Laboratory of Thermo-Fluid Science and Engineering, Ministry of Education, School of Energy and Power Engineering, Xi'an Jiaotong University, Xi'an, 710049, China
*Corresponding author email: wangxp@xjtu.edu.cn

Received: 21.11.2025; revised: 07.05.2026; accepted: 10.08.2026

Abstract

Due to the extremely low ozone depletion potential and global warming potential, 3,3,3-trifluoropropene (R1243zf) is considered a good substitute for traditional hydrofluorocarbons used in vapour-compression refrigeration cycles. The phase behaviour of refrigerant with lubricant oil is a critical factor affecting the performance of the cycle. However, comprehensive analysis of phase behaviour of R1243zf/lubricant oil mixture and quantitative assessment of its impact on the cycle efficiency is still lacking. Therefore, this work employs the Soave-Redlich-Kwong (SRK) equation of state, combined with the modified van der Waals-Berthelot mixing rule and hypothetical oil model proposed by Yokozeki, to investigate the phase equilibrium data of R1243zf/oil mixtures and the phase behaviour of R1243zf with different lubricant oils. Furthermore, the impact of oils on the performance of the vapour-compression refrigeration cycle is quantitatively analysed. Results show that polyolester (POE)-type lubricant oils exhibit superior performance in R1243zf-based refrigeration systems.

Keywords: R1243zf; SRK equation; Lubricant oils; Phase behaviour; Coefficient of performance

Vol. 47(2026), No. 3, 253–260; doi: 10.24425/ather.2026.7526

Cite this manuscript as: Jia, H., Dang, W., & Wang, X. (2026). Analysis of phase behaviour of R1243zf/lubricant oil mixtures and its impact on the performance of vapour-compression refrigeration cycle. *Archives of Thermodynamics*, 47(3), 253–260.

1. Introduction

Environmental issues have become a common challenge for the world. The Paris Agreement and the subsequent Glasgow Climate Pact (COP26) have set clear targets for global temperature control and emission reduction. By 2023, COP28 further advanced these efforts by adopting the "Global Cooling Pledge" which explicitly aims to reduce the cooling-related emissions by 68% by 2050 compared to 2022 levels, demonstrating the international community's firm commitment to mitigating climate change. In the refrigeration industry, the refrigerant plays a critical role in environmental protection, and the development and application of low-global warming potential (GWP) refrigerants have become a key direction for technological innovation [1–3].

In the past decade, hydrofluoroolefins (HFOs) have attracted significant attention due to their unique molecular structures and environmentally friendly characteristics. The C=C double bond in HFO molecules promotes rapid reaction with atmospheric OH radicals, substantially shortening their atmospheric lifetime [4]. Among the various HFOs proposed, 3,3,3-trifluoropropene (R1243zf) garnered widespread interest due to its excellent properties. R1243zf has an ODP of 0 and GWP of 0.82, and extremely short atmospheric lifetime of only 6 days [5,6]. From a thermodynamic perspective, the properties of R1243zf are

very similar to those of R134a, indicating strong replacement compatibility and application potential. Experimental studies have confirmed that, in air conditioning systems, R1243zf exhibits a higher coefficient of performance (COP) and operates with lower suction and exhaust pressures compared to conventional refrigerants [7], making it a promising candidate for the next generation of refrigerants.

It is well known that the thermo-physical properties of R1243zf as well as R1243zf/lubricant oil mixture are essential for the design and optimisation of the vapour compression refrigeration cycle. A series of studies have been reported on the properties of R1243zf, such as critical properties, density, vapour pressure, specific heat capacity and surface tension [8–11]. In addition, the vapour-liquid equilibrium data of R1243zf with lubricant oils were also reported [12–14]. However, a comprehensive analysis of phase behaviour of R1243zf/lubricant oil is still lacking in the literature.

Furthermore, the selection of lubricant oil significantly affects the performance of a refrigeration system because it directly influences oil circulation and refrigerant distribution within the cycle. For example, Chen et al. [15] experimentally compared the effects of different lubricant oils, including polyalkylene glycol (PAG) and mineral oil (MO), in a 1.5 HP R290 split-type room air conditioner. They found that the use of PAG can reduce the amount of R290 in the compressor and improve heating capacity. However, due to the increased viscosity of R290/lubricant oil mixture in the oil sump, the coefficient of performance (COP) under heating conditions is relatively low. Li et al. [16] experimentally analysed the flow characteristics and the impact of lubricant oil in heat pump systems and heat exchangers, pointing out that the oil circulation rate is directly affected by the compressor oil charge. At the same time, oil retention in the evaporator and condenser increases the amount of oil held in the system, impairing heat transfer capacity and consequently degrading overall system performance. Naseri et al. [17] identified that for a modified revolving vane expander in a micro-scale organic Rankine cycle, an oil circulation rate (OCR) of about 1% represents an optimal compromise. Albà et al. [18] employed the Statistical Associating Fluid Theory (SAFT) equation of state to evaluate the performance of lubricants such as PEC5 (pentaerythritol tetrapentanoate) and TrEGDME (triethylene glycol dimethyl ether) in a low-GWP R513A refrigeration cycle, demonstrating that PEC5 had the least impact on cycle efficiency and is more suitable for this system. Therefore, it is necessary to conduct a performance analysis of R1243zf and lubricant oils for the purpose of selecting an appropriate lubricant oil.

In this work, based on the experimental vapour-liquid equilibrium (VLE) data of R1243zf with two mineral oils (3GS and 4GS) and one polyol ester oil (RL68H) [14] mixtures, the SRK equation of state, the modified van der Waals-Berthelot mixing rule, and the hypothetical oil (UniOIL) model proposed by Yokozeki [19] were employed to correlate the data. The phase behaviour of R1243zf with lubricant oils was investigated, and the impact of oil type on the performance of the vapour-refrigeration cycle was evaluated. This work provides a theoretical foundation for deepening the understanding of phase behaviour in R1243zf/lubricant oils and for optimising the refrigeration system.

2. Modelling

In this work, the SRK equation of state along with the van der Waals-Berthelot mixing rule was employed to correlate the experimental VLE data. In addition, due to the lack of critical parameters for the lubricant oil, the hypothetical oil (UniOIL) model proposed by Yokozeki [19] was used. In the UniOIL model, the oil is treated as a single pseudo-pure component with fixed critical temperature and pressure. The SRK equation is defined as follows [20]:

$$P = \frac{RT}{v-b} - \frac{a(T)}{v(v+b)}, \tag{1}$$

where a(T) is the attraction parameter and b is the co-volume parameter. The two parameters are calculated by:

$$a(T) = 0.427480\frac{(RT_c)^2}{P_c}\alpha(T), \tag{2}$$

$$b = 0.08664\frac{RT_c}{P_c}, \tag{3}$$

where R is the gas constant (8.31445 J/(mol·K)), T_c and P_c are the critical temperature (in K) and critical pressure (in Pa) of the R1243zf or lubricant oils, respectively. For R1243zf, the critical temperature and pressure are obtained from REFPROP [21]. Based on the UniOil model, the critical temperature and pressure of the lubricant oils are set to 800 K and 0.95 MPa [19], respectively. a(T) is a temperature-dependent term, defined by the following expressions:

$$\alpha(T) = \sum_{k=0}^{\leq 3}\beta_k(1/T_r - T_r)^k, \quad \text{for } T_r \leq 1, \tag{4}$$

$$\alpha(T) = \beta_0 + \beta_1[\exp(2(1-T_r)) - 1], \quad \text{for } T_r \geq 1. \tag{5}$$

where T_r is the reduced temperature ($T_r = T/T_c$). The value of $\beta(k)$ for R1243zf was determined from regression of vapour density data, and the values for the refrigerant and lubricant oil are provided in Table 1.

Table 1. Values of coefficient $\beta(k)$ in Eq. (4).

Components	β_1	β_2	β_3	β_4
R1243zf	1.0	0.48044	-0.11435	0.04702
Lubricant oil	1.0	1.0	0.0	0.0

In the modified van der Waals-Berthelot mixing rule, the attraction parameter $a(T)$ and co-volume parameter b of the mixtures are obtained by combining the pure-component parameters $a_i(T)$ and b_i through binary interaction parameters. The expressions are given as follows [19]:

$$a = \sum_{i,j=1}^{N}\sqrt{a_i a_j}\, f_{ij}(T)(1-k_{ij})x_i x_j, \tag{6}$$

$$b = \frac{1}{2}\sum_{i,j=1}^{N}(b_i + b_j)\,(1-k_{ij})(1-m_{ij})x_i x_j, \tag{7}$$

$$f_{ij}(T) = \tau_{0,ij} + \tau_{1,ij}/T + \tau_{2,ij}T, \quad (8)$$

$$k_{ij} = \frac{l_{ij}l_{ji}(x_i+x_j)}{l_{ji}x_i+l_{ij}x_j}, \quad (9)$$

where the m_{ij}, l_{ij}, l_{ji}, $\tau_{0,ij}$, $\tau_{1,ij}$ and $\tau_{2,ij}$ are binary interaction parameters, whose values were regressed from binary VLE data. The other parameters obey the relations: $f_{ij} = f_{ji}$, $f_{ii} = 1$, $m_{ij} = m_{ji}$, $m_{ii} = 0$, $k_{ij} = k_{ji}$, $k_{ii} = 0$.

In phase equilibrium calculations, the fugacity coefficient is indispensable – for component i, it is given by Eq. (10); a'_i and b'_i represent the partial derivatives of the attraction and co-volume terms with respect to the mole number of component i, respectively. The expressions are defined in Eqs. (11) and (12).

$$\ln\phi_i = \ln\frac{RT}{P(V-b)} + b'_i\left(\frac{1}{V-b} - \frac{a}{RTb(V+b)}\right) + \frac{a}{RTb}\left(\frac{a'_i}{a} - \frac{b'_i}{b} + 1\right)\ln\frac{V}{V+b}, \quad (10)$$

$$a'_i = 2\sum_{j=1}^{N}\sqrt{a_i a_j}\, f_{ij}x_j\left\{1 - k_{ij} - \frac{l_{ij}l_{ji}(l_{ij}-l_{ji})x_i x_j}{(l_{ji}x_i - l_{ij}x_j)^2}\right\} - a, \quad (11)$$

$$b'_i = \sum_{j=1}^{N}(b_i + b_j)(1 - m_{ij})\, x_j\left\{1 - k_{ij} - \frac{l_{ij}l_{ji}(l_{ij}-l_{ji})x_i x_j}{(l_{ji}x_i - l_{ij}x_j)^2}\right\} - b. \quad (12)$$

The phase equilibrium of the components is defined by the following equation:

$$x_i^{\alpha}\phi_i^{\alpha} = x_i^{\beta}\phi_i^{\beta} = x_i^{\gamma}\phi_i^{\gamma} = \ldots\ldots, (i = 1, \ldots, N), \quad (13)$$

where i is a component, and α, β, γ denote the coexisting phases.

The accuracy of the model was assessed by average absolute relative deviation (AARD) and maximum absolute relative deviation (MARD), which are given by:

$$\mathrm{AARD}/\% = \frac{100}{N}\sum_{i=1}^{N}\left|\frac{p_i^{\mathrm{cal}} - p_i^{\mathrm{exp}}}{p_i^{\mathrm{exp}}}\right|, \quad (14)$$

$$\mathrm{MARD}/\% = \max\left(100\left|\frac{p_i^{\mathrm{cal}} - p_i^{\mathrm{exp}}}{p_i^{\mathrm{exp}}}\right|\right), \quad (15)$$

where N denotes the total number of experimental points; p_i^{cal} and p_i^{exp} represent the calculated and experimental equilibrium pressures of R1243zf, respectively.

3. Results and analysis

3.1. VLE correlation results for R1243zf and three lubricant oils

The optimised binary interaction parameters are summarised in Table 2. Figure 1 illustrates the relative deviations between the calculated and experimental equilibrium pressures.

Table 2. Correlated binary interaction parameters for R1243zf/lubricant oils.

Parameters	R1243zf + 3GS	R1243zf + 4GS	R1243zf + RL68H
m_{ij}	-1.1224×10^{-2}	-1.0934×10^{-1}	-6.6252×10^{-3}
l_{ij}	-4.3360×10^{-3}	1.2181×10^{-1}	7.2919×10^{-2}
l_{ji}	-1.4472×10^{-2}	8.7517×10^{-2}	6.4677×10^{-4}
$\tau_{0,ij}$	4.3596×10^{-1}	4.9923×10^{-1}	7.1982×10^{-1}
$\tau_{1,ij}$	77.4473	72.7367	31.0292
$\tau_{2,ij}$	7.3489×10^{-4}	7.2135×10^{-4}	3.5786×10^{-4}
AARD/%	1.02	1.52	1.49
MARD/%	4.80	7.01	8.24

The AARD for R1243zf mixtures with 3GS, 4GS and RL68H is 1.02%, 1.52% and 1.49%, respectively, demonstrating a good overall quantitative agreement between the SRK model and experimental data.

It can be observed from Fig. 1 that the maximum relative deviations consistently occur at low liquid-phase mole fractions of R1243zf. The MARD for the equilibrium pressure of R1243zf+3GS, R1243zf+4GS and R1243zf+RL68H mixtures is 4.80%, 7.01%, and 8.24%, respectively.

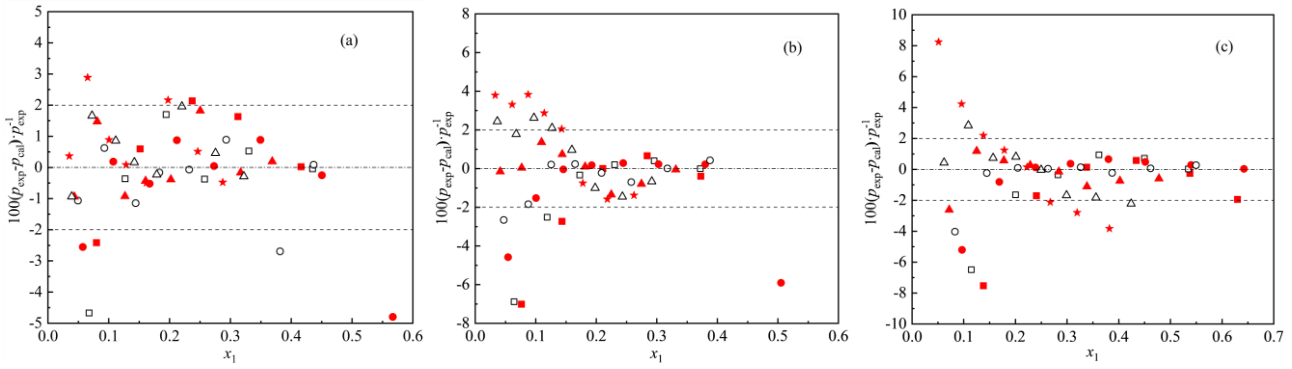


Fig. 1. Relative deviation between experimental data and model calculations of (a) R1243zf/3GS, (b) R1243zf/4GS and (c) R1243zf/RL68H. ■ 283.15 K; □ 293.15 K; ● 303.15 K;○ 313.15 K; ▲ 323.15 K; △ 333.15 K; □ 343.15 K.

3.2. Phase behaviour analysis of R1243zf/lubricant oils

The developed model for the studied R1243zf/oil mixtures was employed to analyse the phase diagrams and critical properties. Initially, the model was used to predict the vapour-liquid-liquid phase equilibrium (VL_1L_2E) and immiscibility regions (L_1L_2E). It should be noted that, due to the significant difference in molar mass between R1243zf and lubricant oils, using the mole fraction x as the abscissa in the phase diagram may result in overly compressed changes in the peripheral regions. Therefore, the mass fraction w was adopted for plotting the phase diagrams.

Figure 2 presents the pressure-temperature-composition ($P-T-w$) phase diagrams for R1243zf mixed with 3GS, 4GS and RL68H oils. Within the temperature range of 283.15−343.15 K, the binary mixtures of R1243zf with three lubricant oils present consistent phase behaviour. The diagrams show two vapour-liquid equilibrium regions (VL_1E and VL_2E), one liquid-liquid equilibrium region (L_1L_2E), and one vapour-liquid-liquid phase equilibrium region (VL_1L_2E), as indicated in Fig. 2. Here, V denotes the vapour phase of R1243zf; L_1 and L_2 represent the oil-rich liquid phase and the R1243zf-rich liquid phase, respectively.

To further investigate the temperature-dependent phase behaviour of the R1243zf/lubricant oils, the phase diagrams of R1243zf/3GS mixture were predicted at three representative temperatures: 343.15 K, 373.15 K and 383.15 K. The three temperatures correspond to conditions below, near and above the critical point of R1243zf. Figure 3 presents the pressure composition ($P-w$) and pressure-molar density ($P-\rho$) diagrams for the binary mixture at 343.15 K. In both diagrams, the L_1L_2E region exhibits a "chimney" shape. However, the width of this chimney shows opposite trends with the increasing pressure in the two types of diagrams. In the $P-w$ diagram, the narrowing of the chimney width is attributed to pressure-induced changes in the mixture's composition distribution. Conversely, in the $P-\rho$ diagram, the broadening of the L_1L_2E region suggests that the increased pressure enhances molecular interactions, thereby expanding the composition range for the liquid-liquid phase region.

Figure 4 presents the $P-w$ and $P-\rho$ diagrams of the R1243zf/3GS mixture at 373.15 K. A clear transformation is observed in the L_1L_2E region compared to 343.15 K. In the $P-w$ diagram, the L_1L_2E region no longer exhibits the upright chimney shape; instead, the L_1 and L_2 phases converge with rising pressure and merge near 10.1 MPa. In the $P-\rho$ diagram,

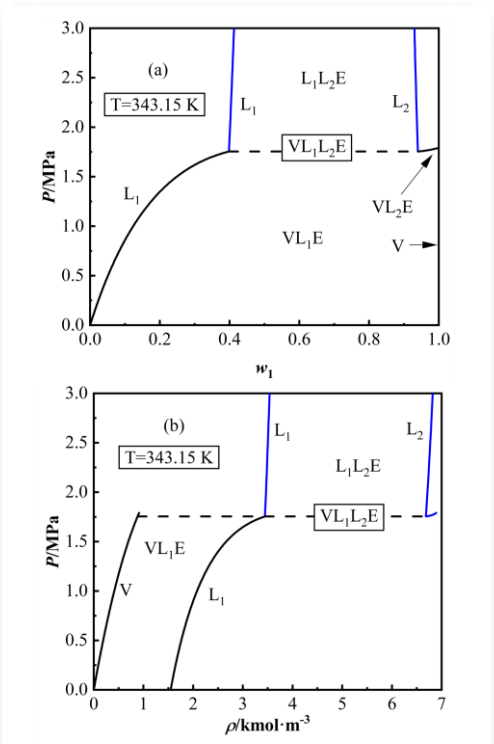


Fig. 3. (a) $P-w$ diagram and (b) $P-\rho$ diagram of the R1243zf/3GS mixture at 343.15 K.

the L_2 phase displays a distinctly different trend in molar density. At low liquid-phase mole fractions of R1243zf, the L_2 curve initially shifts toward higher density before reversing direction. This behaviour becomes particularly evident upon entering the VL_2E region, where the L_2 phase shows a strong tendency to approach the V phase.

Figure 5 shows the $P-w$ and $P-\rho$ diagrams for R1243zf/3GS mixture at 383.15 K. At this condition, the VL_1L_2E and VL_2E phase regions are no longer present. Only the VL_1E vapour-liquid equilibrium and the L_1L_2E liquid-liquid equilibrium persist in the diagrams. These regions are separated by an isopleth located at approximately 3.2 MPa. Below this pressure, the system exhibits vapour-liquid equilibrium, comprising the vapour phase V and the liquid phase L_1. Above 3.2 MPa, liquid-liquid equilibrium prevails, where the L_1 and L_2 phases gradually converge with increasing pressure and eventually merge at the critical point located near 7.98 MPa.

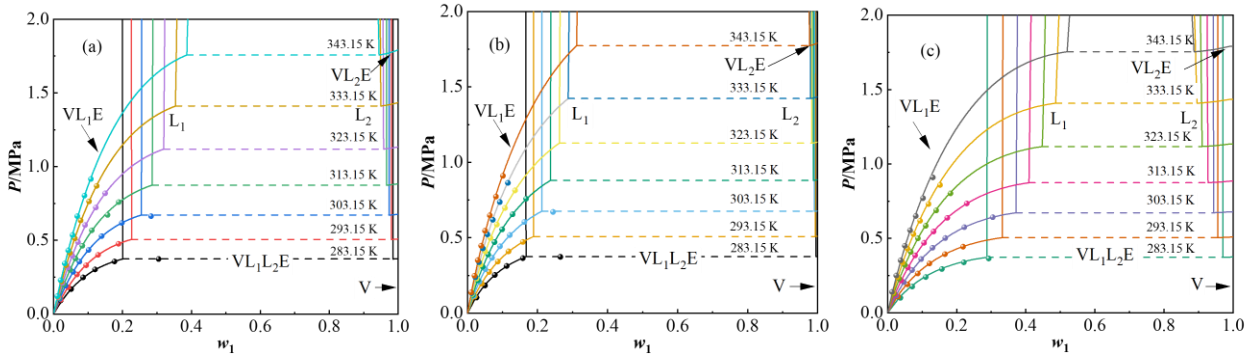


Fig. 2. $P-T-w$ diagrams for R1243zf with three lubricant oils including (a) R1243zf/3GS, (b) R1243zf/4GS and (c) R1243zf/RL68H.

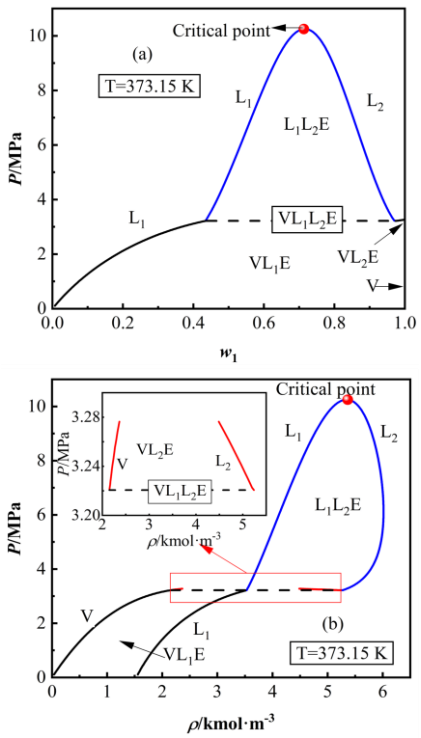


Fig. 4. (a) *P*–*w* diagram and (b) *P*–*ρ* diagram of the R1243zf/3GS mixture at 373.15 K.

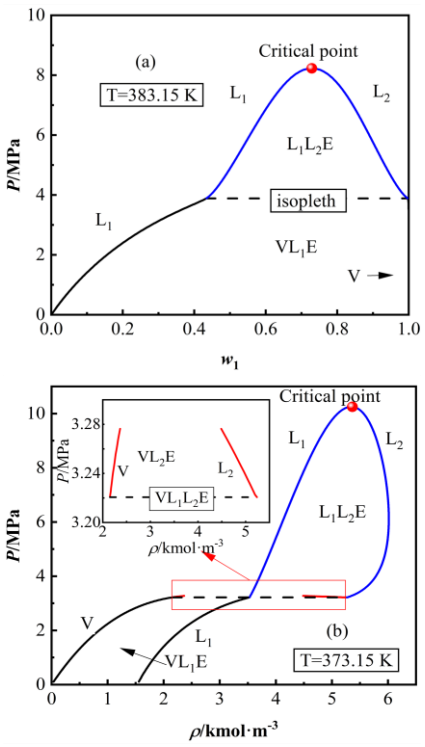


Fig. 5. (a) *P*–*w* diagram and (b) *P*–*ρ* diagram of the R1243zf/3GS mixture at 383.15 K.

Van Konynenburg and Scott [22,23] pioneered the classification of phase behaviour types in binary mixtures, identifying five of the six major phase behaviours. Among these, type III mixture is one of the most extensively studied. Type III mixture is characterised by features including a three-phase equilibrium region, an upper critical solution temperature, and the absence of a lower critical solution temperature. Based on the analysis of *P*–*w* and *P*–*ρ* diagrams at different temperatures, the R1243zf/3GS can be classified as a type III mixture. It should be noted that the mixtures of R1243zf/4GS and R1243zf/RL68H exhibit similar trends with that of R1243zf/3GS and are also categorised as type III mixtures, therefore, the phase diagram of R1243zf/4GS and R1243zf/RL68H mixtures was not discussed here.

The classification of all three R1243zf/oil systems as type III mixtures implies the existence of a three-phase (VL_1L_2) region and a liquid-liquid immiscibility gap under conditions relevant to refrigeration cycles. Among the studied oils, the phase diagrams indicate that RL68H exhibits an immiscibility region that is relatively narrower and shifted compared to the mineral oils 3GS and 4GS. This suggests a lower tendency for phase separation.

3.3. Performance analysis of vapour-compression refrigeration cycle with lubricant oil

In this part, the influence of lubricant oil on the performance of the vapour-compression refrigeration cycle was analysed. The cycle incorporated superheating and subcooling, each set to 2.5 K, to secure a fully condensed liquid after the condenser and to prevent liquid entrainment in the vapour stream entering the compressor. Figure 6 presents the pressure-enthalpy (*P*–*h*) and temperature-entropy (*T*–*s*) diagrams of the vapour-compression refrigeration cycle.

In this study, the coefficient of performance (COP) of the refrigeration cycle was simulated by maintaining a fixed condensing temperature of 330 K. To facilitate quantitative analysis, pressure drops during evaporation and condensation were assumed to be negligible. Table 3 summarises the process conditions of the cycle adopted in this work. In Table 3, P_i and T_i denote the pressure and temperature at state point *i*, respectively; T_{evap} and T_{cond} represent the evaporating and condensing temperatures of the cycle; $w_{i,oil}$ indicates the liquid-phase mass fraction of the lubricant oil at state point *i*.

COP of the cycle is calculated by the following equation:

$$\mathrm{COP} = \frac{\sum q_{in}}{\sum W_{net,in}} = \frac{h_1 - h_4}{h_2 - h_1} = \frac{h_1 - h_3}{h_2 - h_1}, \tag{16}$$

where q_{in} denotes the evaporator heat absorption, $W_{net,in}$ denotes the net compressor work input, and h_i is the specific enthalpy at state *i*. The expansion process is assumed isenthalpic, giving $h_3 = h_4$.

The specific enthalpy of the R1243zf/lubricant oil mixture at state *i* is determined using the thermodynamic model of Youbi-Idrissi [24], and is given by:

Table 3. Process conditions of the vapour-compression refrigeration cycle for refrigerant/lubricant oil mixture.

Operating point	1	2	3
Degrees of freedom	2	2	2
Fixed variables	P_1, T_{evap}	P_3, S_2	P_3, T_{cond}
Obtained variables	$w_{1,oil}$	T_2, $w_{2,oil}$	$w'_{3,oil}$, $w''_{3,oil}$

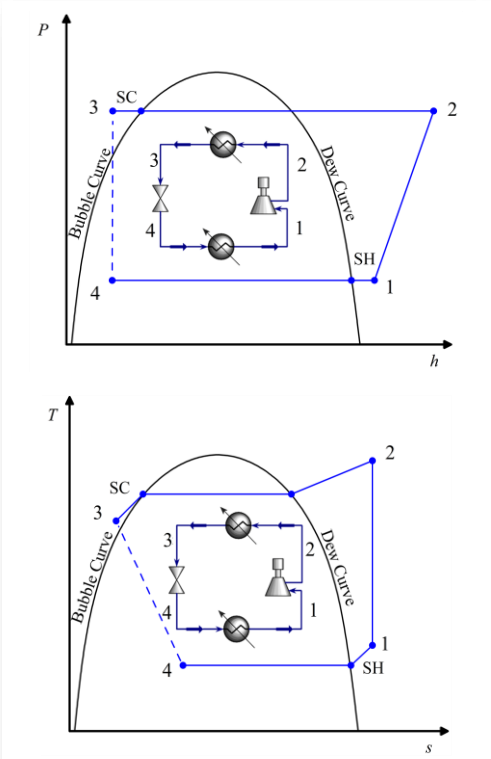


Fig. 6. $P-h$ and $T-s$ diagrams |of the vapour-compression refrigeration cycle.

$$h_i = \left(\frac{m_{L,r}}{m_{L,r}+m_{oil}+m_V}\right) h_{L,r} + \left(\frac{m_V}{m_{L,r}+m_{oil}+m_V}\right) h_V + \left(\frac{m_{oil}}{m_{L,r}+m_{oil}+m_V}\right) h_{oil}, \quad (17)$$

where h_i is the specific enthalpy at state point i (J/kg), $h_{L,r}$ and h_V are the specific enthalpies of the liquid and vapour refrigerant (J/kg), and h_{oil} is the specific enthalpy of the lubricate oil (J/kg). The liquid refrigerant enthalpy $h_{L,r}$ and vapour refrigerant enthalpy h_V were obtained from REFPROP [21]. The specific enthalpy of the lubricating oil (h_{oil}) is expressed as:

$$h_{oil} = h_{ref} + \int_{T_{ref}}^{T} C_{P,oil}\, \mathrm{d}T, \quad (18)$$

where h_{ref} is the reference specific enthalpy (J/kg), T_{ref} is the reference temperature (K), and $C_{p,oil}$ is the specific heat capacity of the lubricate oil (J/(kg·K)). Since only enthalpy differences between state points are relevant for efficiency calculations, it is sufficient to maintain consistent values of T_{ref} and h_{ref} for the lubricant across all states. Here, T_{ref} is taken as 273.15 K and h_{ref} as 0 J/kg. The specific heat capacity of the lubricate oil, $C_{p,oil}$ can be calculated using the model proposed by Liley et al. [25]:

$$C_{p,oil} = 4.186\left[\frac{0.388+0.00045(1.8T+32)}{\sqrt{\rho_{oil}/998.5}}\right] = \frac{(1.684+0.0034T)}{\sqrt{\rho_{oil}/998.5}}, \quad (19)$$

where ρ_{oil} is the density of the lubricate oil (kg/m^3) at 288.71 K.

To investigate the influence of lubricant oil content on cycle performance, COP was evaluated at varying oil circulation rates (OCR), defined as the mass ratio of lubricant oil to the total circulating fluid. Calculations were performed at OCR levels of 1%, 2% and 3%, representing conditions of oil deficiency, normal operation and potential mild compressor leakage, respectively.

Figure 7 presents the calculated COP values for mixtures of R1243zf with 3GS, 4GS and RL68H under different OCR values. It indicates that at a constant evaporation temperature, the COP exhibits a clear decreasing trend as OCR increases. For example, at an evaporation temperature of 278 K, as OCR increases from 1% to 3%, the COP for the R1243zf/3GS mixture decreases from 3.92 to 3.34, representing a reduction of 14.80%. These findings are consistent with the results reported by Albà et al. [18] for R513A/lubricant systems, where COP was also found to decrease with increasing oil circulation rate.

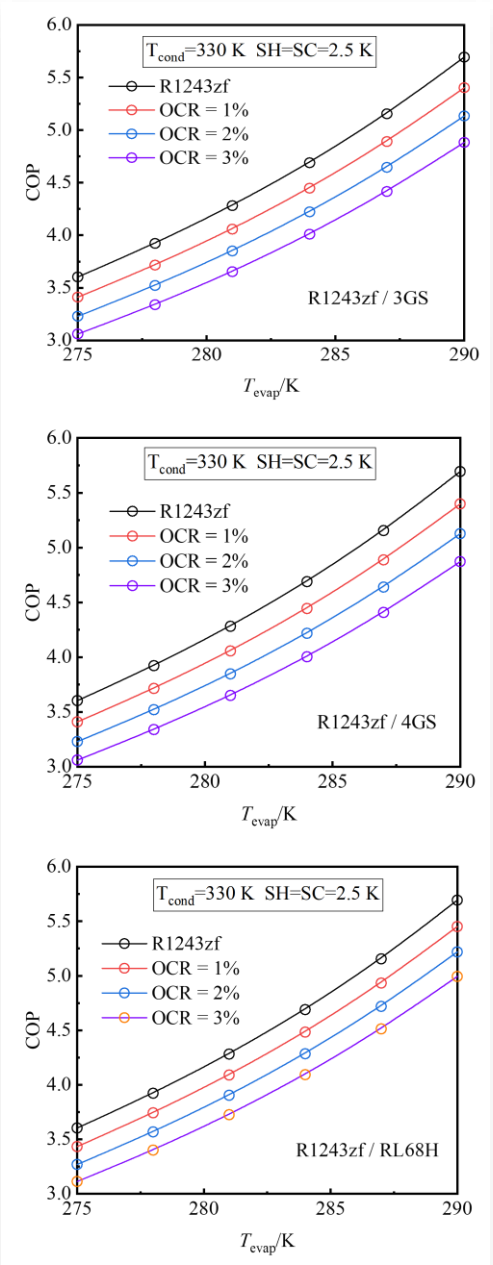


Fig. 7. COP of R1243zf/3GS, R1243zf/4GS and R1243zf/RL68H mixtures under different OCR.

Figure 8 shows the reduction in COP of the refrigeration cycle using R1243zf/oil mixture compared to that of pure R1243zf. As shown in the figure, the COP reduction exhibits a clear increasing trend with rising OCR. At a low OCR of 1% and evaporation temperature of 278 K, the COP reductions are 0.207, 0.208 and 0.180 for 3GS, 4GS and RL68H, respectively. At a high OCR of 3% under the same evaporation temperature, the corresponding reductions are 0.582, 0.583 and 0.522. This trend occurs because a higher OCR increases the proportion of lubricant in the system, which correspondingly displaces the refrigerant and reduces the effective mass flow rate contributing to refrigeration, thereby diminishing the cooling capacity.

At a fixed OCR, the negative impact of the lubricant oil on the system efficiency becomes more pronounced as the evaporation temperature increases, as indicated in Fig. 8. For example, at an OCR of 3% for R1243zf/3GS mixture, the COP reduction increases from 0.542 at 275 K to 0.81 at 290 K. Moreover, the extent of COP reduction varies among different lubricants. Particularly, under lower evaporation temperature, RL68H shows the smallest adverse effect on cycle efficiency compared to the other two lubricants.

At OCR of 3% and evaporation temperature of 278 K, the COP reduction for RL68H is 10.4% lower than that for 3GS, and 10.6% lower than that for 4GS. Therefore, from a system performance perspective, RL68H is identified as the most suitable lubricant for R1243zf refrigeration systems among the three candidates. This conclusion is consistent with the work of Albà et al. [18], who employed the polar soft-SAFT equation of state to evaluate lubricants for R513A, and identified PEC5 (a pure component of POE oil) as the optimal choice, with a COP decrease of less than 3% across the studied range.

RL68H is a POE type lubricant, whereas 3GS and 4GS are mineral oils. The superior performance of R1243zf/RL68H mixture can be attributed to its molecular structure. The oxygen-containing ester linkages in POE lubricant provide favourable polar interactions with fluorinated R1243zf molecules, enhancing miscibility, giving more stable thermodynamic behaviour.

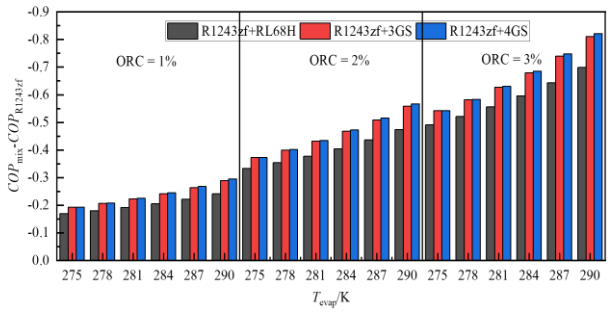


Fig. 8. Reduction in COP for R1243zf/3GS, R1243zf/4GS and R1243zf/RL68H mixtures compared to pure R1243zf.

4. Conclusions

This study correlated the experimental phase equilibrium data of R1243zf with three lubricant oils using the SRK equation of state, modified van der Waals-Berthelot mixing rule and the UniOIL model proposed by Yokozeki. The relative deviations between calculated and experimental values were predominantly within ±2%. The correlated model was subsequently applied to predict and analyse phase behaviour, including vapour-liquid and liquid-liquid equilibrium of R1243zf/lubricant oils. Phase diagram analysis confirmed that the binary systems of R1243zf with 3GS, 4GS and RL68H are classified as type III mixtures. Furthermore, the coefficient of performance (COP) of the cycle was comprehensively evaluated. By comparing the effects of different lubricants on cycle performance, it can be concluded that RL68H is the most suitable lubricant among the three lubricants for R1243zf refrigeration systems. The modelling framework and COP evaluation methodology developed in this work can be extended to a broader range of refrigerant/lubricant combinations, providing a useful basis for lubricant screening.

Acknowledgements

This work was supported by National Natural Science Foundation of China (Grant No. 52276165).

References

[1] Esen, M. (2004). Thermal performance of a solar cooker integrated vacuum-tube collector with heat pipes containing different refrigerants. *Solar Energy*, 76(6), 751–757. doi: 10.1016/j.solener.2003.12.009

[2] Esen, M., Hazar, H., & Esen, H. (2005). Experimental investigation of a solar cooker using collector with heat pipes. *Sigma Journal of Engineering and Natural Sciences*, 23(1), 114–122.

[3] Esen, M., & Esen, H. (2005). Experimental investigation of a two-phase closed thermosyphon solar water heater. *Solar Energy*, 79(5), 459–468. doi: 10.1016/j.solener.2005.01.001

[4] Wallington, T.J., Andersen, M.S., & Nielsen, O.J. (2015). Atmospheric chemistry of short-chain haloolefins: Photochemical ozone creation potentials (POCPs), global warming potentials (GWPs), and ozone depletion potentials (ODPs). *Chemosphere*, 129, 135–141. doi: 10.1016/j.chemosphere.2014.06.092

[5] Bobbo, S., Di Nicola, G., Zilio, C., Brown, J.S., & Fedele, L. (2018). Low GWP halocarbon refrigerants: A review of thermophysical properties. *International Journal of Refrigeration*, 90, 181–201. doi: 10.1016/j.ijrefrig.2018.03.027

[6] McLinden, M.O., Kazakov, A.F., Brown, J.S., & Domanski, P.A. (2014). A thermodynamic analysis of refrigerants: Possibilities and tradeoffs for low-GWP refrigerants. *International Journal of Refrigeration*, 38, 80–92. doi: 10.1016/j.ijrefrig.2013.09.032

[7] Lai, N.A. (2014). Thermodynamic properties of HFO-1243zf and their application in study on a refrigeration cycle. *Applied Thermal Engineering*, 70(1), 1–6. doi: 10.1016/j.applthermaleng.2014.04.042

[8] Brown, J.S., Di Nicola, G., Fedele, L., Bobbo, S., & Zilio, C. (2013). Saturated pressure measurements of 3,3,3-trifluoroprop-1-ene (R1243zf) for reduced temperatures ranging from 0.62 to 0.98. *Fluid Phase Equilibria*, 351, 48–52. doi: 10.1016/j.fluid.2012.09.036

[9] Higashi, Y., & Sakoda, N. (2018). Measurements of PvT properties, saturated densities, and critical parameters for 3,3,3-trifluoropropene (HFO1243zf). *Journal of Chemical and Engineering Data*, 63(10), 3818–3822. doi: 10.1021/acs.jced.8b00452

[10] Di Nicola, G., Brown, J.S., Fedele, L., Securo, M., Bobbo, S., & Zilio, C. (2013). Subcooled liquid density measurements and PvT measurements in the vapor phase for 3,3,3-trifluoroprop-1-ene (R1243zf). *International Journal of Refrigeration*, 36(8), 2209–2215. doi: 10.1016/j.ijrefrig.2013.08.004

[11] Kondou, C., Nagata, R., Nii, N., Koyama, S., & Higashi, Y. (2015). Surface tension of low GWP refrigerants R1243zf, R1234ze(Z), and R1233zd(E). *International Journal of Refrigeration*, 53, 80–89. doi: 10.1016/j.ijrefrig.2015.01.005

[12] Luo, Y., Liu, Z., Lu, C., & Wang, X. (2022). Vapor-liquid equilibrium measurements of 3,3,3-trifluoropropene with pentaerythritol tetraheptanoate and pentaerythritol tetranonanoate. *The Journal of Chemical Thermodynamic*s, 174, 106874. doi: 10.1016/j.jct.2022.106874

[13] Luo, Y., Wang, X., & Wang, X. (2023). Solubilities of 3,3,3-trifluoropropene in pentaerythritol tetrahexanoate and pentaerythritol tetraoctanoate from 278.15 K to 343.15 K at pressures to 1 MPa. *Fluid Phase Equilibria*, 566, 113699. doi: 10.1016/j.fluid.2022.113699

[14] Jia, H., Wang, X., & Wang, X. (2023). Vapor-liquid equilibrium of 3,3,3-trifluoropropene with mineral oils and POE lubricant between 283.15 K and 343.15 K. *International Journal of Refrigeration*, 146, 375–380. doi: 10.1016/j.ijrefrig.2022.11.027

[15] Chen, R., Wu, J., & Duan, J. (2019). Performance and refrigerant mass distribution of a R290 split air conditioner with different lubricating oils. *Applied Thermal Engineering*, 162, 114225. doi: 10.1016/j.applthermaleng.2019.114225

[16] Li, K., Kong, F., Luo, S., Liu, N., Zhang, H., Dou, B., Zhao, Y., Zhou, X., Tu, R., Su, L., & He, Q. (2024). Influence of lubricating oil circulation characteristics on the performance of electric vehicle heat pump system under low temperature conditions. *Applied Thermal Engineering*, 236, 121601. doi: 10.1016/j.applthermaleng.2023.121601

[17] Naseri, A., Moradi, R., Cioccolanti, L., & Subiantoro, A. (2023). Impact of the lubricant on a modified revolving vane expander (M-RVE) in an organic Rankine cycle system. *Energies*, 16(14), 5340. doi: 10.3390/en16145340

[18] Albà, C.G., Llovell, F., & Vega, L.F. (2021). Searching for suitable lubricants for low global warming potential refrigerant R513A using molecular-based models: Solubility and performance in refrigeration cycles. *International Journal of Refrigeration*, 128, 252–263. doi: 10.1016/j.ijrefrig.2021.04.010

[19] Yokozeki, A. (2001). Solubility of refrigerants in various lubricants. *International Journal of Thermophysics*, 22(4), 1057–1071. doi.: 10.1023/A:1010695705260

[20] Soave, G. (1972). Equilibrium constants from a modified Redlich-Kwong equation of state. *Chemical Engineering Science*, 27(6), 1197–1203. doi: 10.1016/0009-2509(72)80096-4

[21] Lemmon, E.W., Bell, I.H., Huber, M.L., & McLinden, M.O. (2019). *NIST Standard Reference Database 23: Reference fluid thermodynamic and transport properties-REFPROP* (*Version 10.0*). National Institute of Standards and Technology. https://pages.nist.gov/REFPROP-docs/ [accessed 10 Oct. 2025].

[22] Scott, R.L., & Van Konynenburg, P.H. (1970). Static properties of solutions. Van der Waals and related models for hydrocarbon mixtures. *Discussions of the Faraday Society*, 49, 87–97. doi: 10.1039/DF9704900087

[23] Van Konynenburg, P.H., & Scott, R.L. (1980). Critical lines and phase equilibria in binary van der Waals mixtures. *Philosophical Transactions of the Royal Society A: Mathematical, Physical and Engineering Sciences*, 298(1442), 495–540. doi: 10.1098/rsta.1980.0266

[24] Youbi-Idrissi, M., Bonjour, J., Marvillet, C., & Meunier, F. (2003). Impact of refrigerant–oil solubility on an evaporator performance working with R-407C. *International Journal of Refrigeration*, 26(3), 284–292. doi: 10.1016/S0140-7007(02) 00129-9

[25] Mermond, Y., Feidt, M., & Marvillet, C. (1999). Thermodynamic and physical properties of mixtures of refrigerants and oils. *International Journal of Refrigeration*, 22(7), 569–579. doi: 10.1016/S0140-7007(99)00015-8